BAOJ Biotechnology

Kal Renganathan Sharma, BAOJ Biotech 2016, 2: 2
2: 015

Review

On Convexo Concave Concentration Profile, Time Lag before Formation, Occurrence of Maxima and Attainment of Asymptotic Plateau during Pyrolysis of Cellulose

Kal Renganathan Sharma[1*]

[1]*HCC Global Energy Institute 555 Community College Drive Suite USA*

Abstract

Computer simulations are used to study the kinetics of reactions that occur during pyrolysis of cellulose. The scheme of reactions that are believed to occur during pyrolysis of cellulose is given in Figure 1.0. The scheme of reactions used in the computer simulation is shown in Figure 1.0. The kinetic rate expressions of the reactions shown in Figure 1.0 are given by Eqs. (1-6) the kinetic rate equations given by Eqs. (1-6) were made dimensionless for the six species and seven reaction rate constants. The state-space model for kinetic rate expressions is given by Eq. (14). The Eigen values are 0 thrice: $-(\varepsilon+\gamma)$, $-(\beta+\delta+\kappa)$, $-(1+\omega)$. Negative signs for Eigen values indicate a stable system. Eqs. (8-1) can be solved for by the method of Laplace transforms. The model solutions are given by Eqs. (23-28). The product distributions are shown in Figure 2.0 for a typical set of reaction rate constants. The intermediate product species, activated cellulose, R, and primary tar, S, can be seen to undergo a maximum concentration as a function of time. The concentration profile of species S is seen to be convexo-concave during the early times of formation. The secondary tar and secondary gas begin to form after a lag time. The concentration of product P rises and reaches an asymptotic plateau. The dimensionless concentration of species R, S, P, and [T + U] are plotted as a function of conversion of A in Figure 3.0

Keywords: Pyrolysis of Cellulose; Kinetic Scheme; Multiple Reactions; Method of Eigen Vectors and Eigen Values; Method of Laplace Transforms; Product Distribution

Introduction

Biomass fast pyrolysis is the technology used in order to produce liquid fuels such as bio-oil. Bio-oil can be readily transported and stored, used as fuel at thermal power stations, upgraded and combined with refinery products in order to obtain transportation liquid fuels such as gasoline, diesel and or jet fuel. During fast pyrolysis biomass is allowed to undergo a series of thermo chemical reactions and thermal degradation into vapor phase mixture of small molecules of organic compounds and a carbon rich residue called bio-char in an oxygen free environment. Cyclones and air filters are used to separate the vapor mixture from the bio-char. Recent advances made in experimental methods and computer modeling on kinetics of pyrolysis of cellulose is discussed in Antall et al. [1].

Lignocellulosic biomass can be used as feed stock in order to produce chemicals. This is a renewable source and potentially offers solutions for sustainable production. Pyrolysis is a method of conversion of biomass into products such as char, chemicals, bio-oil and syn-gas. It can also be used to fuel stoves. Linear homo polymer of glucopyranose residues linked by β-1,4 glycosidic bonds is present in cellulose which forms 50 wt. % of the lignocellulosic biomass. Pyrolysis studies of cellulose can be found in the literature. Pyrolysis kinetics can be studied either experimentally or by computer simulations. Computer simulations are preferred to close form analytical modeling on account of the seven or more reactions that can be identified during pyrolysis. MS Excel spreadsheet for Windows 2013 can be used and high speed desktop computers can be used in order to obtain solutions to simultaneous ODEs, ordinary differential equations using numerical methods such as RungaKutta that dictates the kinetics of these reactions. The product and other species distributions can be plotted and studied and used in design of gasifier, reactor or pyrolyzer. When does a desired product reach maxima? When does an undesired, toxic species reach a minimal concentration? Is there a cross-over time from then on another species is made more than the desired species? How does the product distribution change with conversion of the starting material? Can temperature be used to change the reaction rate constants in a manner than optimal profit can be realized by the investor? These are some of the questions that will be answered from a study of computer simulations of the kinetics of 5 or more species that can be expected to participate during pyrolysis of cellulose. Diffusion, mass transfer and heat

***Corresponding author:** Kal Renganathan Sharma ,Houston Community College Global Energy Institute 555 Community College Drive, Houston, USA TX 77013, Tel: 281-256-2976 ; E-mail: jyoti_kalpika@yahoo.com

Sub Date: June 30, 2016, **Acc Date:** July 13, 2016, **Pub Date:** July 15, 2016.

Citation: Kal Renganathan Sharma (2016) On Convexo Concave Concentration Profile, Time Lag before Formation, Occurrence of Maxima and Attainment of Asymptotic Plateau during Pyrolysis of Cellulose. BAOJ Biotech 2: 015.

transfer aspects to the process are important as well. But focus is applied to the kinetic information here. Pyrolysis is a thermo chemical conversion of biomass into fuels and chemicals. Scale-up of interesting fuel chemistry can be facilitated using kinetic models. Often time's pilot plants are understaffed and models can replace pilot plant trials.

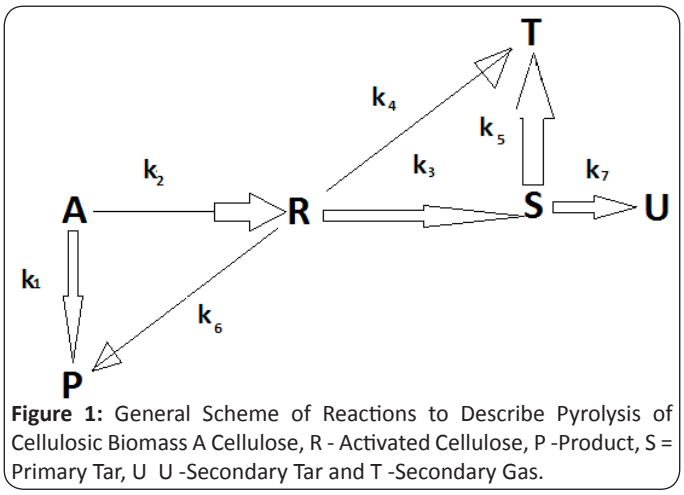

Figure 1: General Scheme of Reactions to Describe Pyrolysis of Cellulosic Biomass A Cellulose, R - Activated Cellulose, P -Product, S = Primary Tar, U U -Secondary Tar and T -Secondary Gas.

The molecular structure at a micro-level, morphological structure at a meso-level and textural structure at a macro-level has been considered for lignocellulosic biomass. The cell wall is now believed to comprise of middle lamella sandwiched between the primary and secondary cell walls. Pectic substances make up the lamella shared with two contiguous cells. Hemicelluloses, pectin's and proteins are the molecules that make the cell walls. Micro fibrillar morphology and interpenetrating network structure can be seen in the cell wall. Cross-linking between cellulosic and non-cellulosic polymers and pectin's has been found to offer structural support to the assembly. Secondary cell walls arise from thickening of primary cell walls and lignin gets included in to the cell wall matrix. Pectin is found to cease depositing [2,3]. Hydrogen bonding between polysaccharide molecules and coalescence of lignin-carbohydrate are not well understood. There were found three macromolecules that the cell wall is made of; (i) cellulose; (ii) hemi-cellulose and; (iii) lignin. Methylation experiments were used in order to confirm the macromolecular structure of cellulose. The repeat unit is D-Glucose, a stereoisomer ($C_6H_{12}O_6$). The repeat units are connected by β-1,4 glucosidic linkages. Supramolecular structures are formed by hydrogen bonds. The molecular weight of the cellulose falls in a range of 54,900 - 2.75 million. The lower end of the range is for rayon fibers and the higher end of the range is for capsule cellulosic products.

Investigators recognized two competitive endothermic reactions during the pyrolysis of cellulose: (i) formation of a hydro cellulose and; (ii) reversible polymerization of the unconverted cellulose into tar. Char and secondary gas are formed from exothermic degradation of anhydrocellulose.

Wooten et. al. [4] proposed a multi-step reaction scheme. Treating the char as product P a general scheme for pyrolysis is shown in Figure 1.0. In Figure1.0, A is the cellulose, R is the activated cellulose, P is the product, S and U are the primary and secondary tar and T is the secondary gas. The secondary char from cellulose is formed from the polymerization of anhydro sugars also called as levoglucosan. Levoglucosan undergoes vapor phase polymerization.

Bai et. al. [5] investigated the chemical events after formation of levoglucosan during cellulose pyrolysis. They used time-resolved thermo gravimetric analysis/differential scanning calorimetric combined with mass spectrometry measurements followed by high performance liquid chromatography and gel filtration chromatography of the pyrolysis residue. They found that levoglucosan formed during cellulose pyrolysis is initially a liquid. Then it underwent simultaneous reaction and mass transfer processes. The mass transfer operation was evaporation and reaction event was polymerization. Levoglucosan that evaporates is removed upon formation from the high temperature pyrolysis zone. Upon transfer it cannot participate in further reaction. Levoglucosan that polymerizes is trapped in the pyrolysis zone. The polyanhydro sugar was found to dehydrate into lower molecular weight products and char. The lower molecular weight product was found to be volatile. The oligosaccharides that form during polymerization are subjected to two simultaneous reaction pathways: direct decomposition to low molecular weight products such as water, carbon dioxide, 5-hydroxymethylfurfural, furfural, furan and acetic acid, and formation of polysaccharides that eventually dehydrate to char and low molecular weight volatiles. Based on the experimental observations and quantitative measurements, a modified cellulose pyrolysis pathway involving levoglucosan as the major intermediate was also suggested. Review of mechanisms and rates of linin and whole biomass pyrolysis was presented by Antal [6]. They discussed the complex sequence of competing solid and vapor phase pyrolysis pathways.

Kinetic Model

The kinetic rate expressions for the scheme of reactions shown in Figure 1.0 are written below. First order rate is assumed for each of the simple, irreversible reactions.

$$r_A = -\left(\frac{dC_A}{dt}\right) = (k_1 + k_2)C_A \quad (1)$$

$$r_P = \left(\frac{dC_P}{dt}\right) = k_1 C_A + k_6 C_R \quad (2)$$

$$r_R = \left(\frac{dC_R}{dt}\right) = k_2 C_A - (k_4 + k_3 + k_6)C_R \quad (3)$$

$$r_S = \left(\frac{dC_S}{dt}\right) = k_3 C_R - (k_5 + k_7)C_S \quad (4)$$

$$r_T = \left(\frac{dC_T}{dt}\right) = k_4 C_R + k_5 C_S \quad (5)$$

$$r_U = \left(\frac{dC_U}{dt}\right) = k_7 C_S \quad (6)$$

The kinetic rate equations given by Eqs. (1-6) can make dimensionless by the following substitutions for the 6 species and

7 reaction rate constants;

$$u_A=\left(\frac{C_A}{C_{A0}}\right);\tau=k_1\tau;u_P=\left(\frac{C_P}{C_{A0}}\right);u_R=\left(\frac{C_R}{C_{A0}}\right);u_S=\left(\frac{C_S}{C_{A0}}\right);u_T=\left(\frac{C_T}{C_{A0}}\right);u_U=\left(\frac{C_U}{C_{A0}}\right)$$

$$\omega=\left(\frac{k_2}{k_1}\right);\kappa=\left(\frac{k_3}{k_1}\right);\delta=\left(\frac{k_4}{k_1}\right);\varepsilon=\left(\frac{k_5}{k_1}\right);\beta=\left(\frac{k_6}{k_1}\right);\gamma=\left(\frac{k_7}{k_1}\right) \quad (7)$$

The dimensionless kinetic rate equations are then seen to be;

$$\left(\frac{du_A}{d\tau}\right)=-(1+\omega)u_A \quad (8)$$

$$\left(\frac{du_P}{d\tau}\right)=u_A+\beta u_R \quad (9)$$

$$\left(\frac{du_R}{d\tau}\right)\ \omega u_A-\ (\beta+\delta+k)u_R \quad (10)$$

$$\left(\frac{du_S}{d\tau}\right)\ Ku_R-(\varepsilon+\gamma)u_S \quad (11)$$

$$\left(\frac{du_t}{d\tau}\right)\delta u_R+\varepsilon u_S \quad (12)$$

$$\left(\frac{du_U}{d\tau}\right)=\gamma u_S \quad (13)$$

State space model expression for the 6 species undergoing reaction can be written in terms of a 6 member vector and a 6 x 6 rate matrix that is sparse.

$$\frac{d}{d\tau}\begin{pmatrix}u_A\\u_P\\u_R\\u_T\\u_S\\u_U\end{pmatrix}=\begin{pmatrix}-(1+\omega)&0&0&0&0&0\\1&0&\beta&0&0&0\\\omega&0&-(\beta+\delta+\kappa)&0&0&0\\0&0&\delta&0&\varepsilon&0\\0&0&\kappa&0&-(\varepsilon+\gamma)&0\\0&0&0&0&\gamma&0\end{pmatrix}\begin{pmatrix}u_A\\u_P\\u_R\\u_T\\u_S\\u_U\end{pmatrix} \quad (14)$$

The stability of the system can be studied by obtaining the Eigen values of the rate matrix.

$$|K-\lambda I|=\begin{pmatrix}-(1+\omega+\lambda)&0&0&0&0&0\\1&-\lambda&\beta&0&0&0\\\omega&0&-(\beta+\delta+\kappa+\lambda)&0&0&0\\0&0&\delta&-\lambda&0&0\\0&0&\kappa&0&-(\varepsilon+\gamma+\lambda)&0\\0&0&0&0&\gamma&-\lambda\end{pmatrix} \quad (15)$$

The characteristic polynomial can be seen to be;

$$\lambda(\varepsilon+\gamma+\lambda)((\lambda)(\beta+\delta+\kappa+\lambda)\lambda(1+\omega+\lambda))=0 \quad (16)$$

The Eigen values are 0 thrice, - (ε+γ), - (β+δ+κ), - (1+ω). Negative sign for Eigen values indicate a stable system. Eqs. (8-13) can be solved for by the method of Laplace transforms. The Laplace transforms of Eqs. (8-13) are taken and the Laplace transformed expressions for each of the 6 species are obtained after elimination of common variable between the equations where they occur. The initial time conditions are $u_A(0) = 1$; $u_P(0) = 0$; $u_R(0) = 0$; $u_S(0) = 0$; $u_T(0)=0$; $u_U(0)=0$. It can be seen that;

$$u_A(s)=\frac{1}{(s+\omega+1)} \quad (17)$$

$$u_R(s)=\frac{\omega}{(s+\omega+1)(s+\beta+\delta+\kappa)} \quad (18)$$

$$u_S(s)=\frac{\omega\kappa}{(s+\omega+1)(s+\beta+\delta+\kappa)(s+\varepsilon+\gamma)} \quad (19)$$

$$u_P(s)=\frac{1}{(s)(s+\omega+1)}+\frac{\beta\omega}{(s+\omega+1)(s+\beta+\delta+\kappa)} \quad (20)$$

$$u_T(s)=\frac{\omega\kappa\varepsilon}{(s)(s+\omega+1)(s+\beta+\delta+\kappa)(s+\varepsilon+\gamma)}+\frac{\omega\delta}{(s)(s+\omega+1)(s+\beta+\delta+\kappa)} \quad (21)$$

$$u_U(s)=\frac{\omega\kappa\gamma}{(s)(s+\omega+1)(s+\beta+\delta+\kappa)(s+\varepsilon+\gamma)} \quad (22)$$

The Laplace transformed expressions are inverted using tables given in Mickley et al. [7] into the time domain and the species concentration as a function of time can be seen to be;

$$u_A(\tau)=e^{-(\omega+1)\tau} \quad (23)$$

$$u_R(\tau)=\left(\frac{\omega}{\beta+\delta+\kappa-\omega-1}\right)\left(e^{-(\omega+1)\tau}-e^{-(\beta+\delta+\kappa)\tau}\right) \quad (24)$$

$$u_P(\tau)=\left(\frac{1-e^{-(\omega+1)\tau}}{(\omega+1)}\right)+\beta\omega\left(\frac{e^{-(\omega+1)\tau}-e^{-(\beta+\delta+\kappa)\tau}}{(\beta+\delta+\kappa-\omega-1)}\right) \quad (25)$$

$$u_S(\tau)=(\omega\kappa)\frac{(\varepsilon+\gamma-\beta-\delta-\kappa)e^{-(\omega+1)\tau}+(\omega+1-\varepsilon-\gamma)e^{-(\beta+\delta+\kappa)\tau}+(\beta+\delta+\kappa-\omega-1)e^{-(\varepsilon+\gamma)\tau}}{(\omega+1-\beta-\delta-\kappa)(\varepsilon+\gamma-\beta-\delta-\kappa)(\omega+1-\varepsilon-\gamma)} \quad (26)$$

$$u_U(\tau)=(\gamma\omega\kappa)\frac{\frac{(\varepsilon+\gamma-\beta-\delta-\kappa)}{(\omega+1)}(1-e^{-(\omega+1)\tau})+\frac{(\omega+1-\varepsilon-\gamma)}{(\beta+\delta+\kappa)}(1-e^{-(\beta+\delta+\kappa)\tau})+\frac{(\beta+\delta+\kappa-\omega-1)}{(\varepsilon+\gamma)}(1-e^{-(\varepsilon+\gamma)\tau})}{(\omega+1-\beta-\delta-\kappa)(\varepsilon+\gamma-\beta-\delta-\kappa)(\omega+1-\varepsilon-\gamma)} \quad (27)$$

$$u_T(\tau)=(\varepsilon\omega\kappa)\frac{\frac{(\varepsilon+\gamma-\beta-\delta-\kappa)}{(\omega+1)}(1-e^{-(\omega+1)\tau})+\frac{(\omega+1-\varepsilon-\gamma)}{(\beta+\delta+\kappa)}(1-e^{-(\beta+\delta+\kappa)\tau})+\frac{(\beta+\delta+\kappa-\omega-1)}{(\varepsilon+\gamma)}(1-e^{-(\varepsilon+\gamma)\tau})}{(\omega+1-\beta-\delta-\kappa)(\varepsilon+\gamma-\beta-\delta-\kappa)(\omega+1-\varepsilon-\gamma)}$$
$$+\left(\frac{\omega\delta}{\beta+\delta+\kappa-\omega-1}\right)\frac{1}{(\omega+1)}\left((1-e^{-(\omega+1)\tau})-\frac{}{(\beta+\delta+\kappa)}(1-e^{-(\beta+\delta+\kappa)\tau})\right) \quad (28)$$

It can be seen that.

$$1=u_A+u_R+u_P+u_S+u_T+u_U \quad (29)$$

The product distributions are shown in Figure 2.0 for a typical set of reaction rate constants.

The reaction rate constant ratios used in the simulation were;

ω	0.9
β	0.4
κ	0.6
δ	0.25
ε	0.33
γ	0.25

Table 1: Reaction Rate Constants for Product Distribution Shown in Figure 2.0

The intermediate product species, activated cellulose, R and primary tar S, can be seen to undergo a maximum concentration as a function of time. The secondary tar and secondary gas begin to form after a lag time. The concentration of product P rises and reaches an asymptotic plateau.

The dimensionless concentration of species R, S, P and T+U is plotted as a function of conversion of A in Figure 3.0. The reaction rate constants used in the computer simulation to generate Figure 3.0 are as follows;

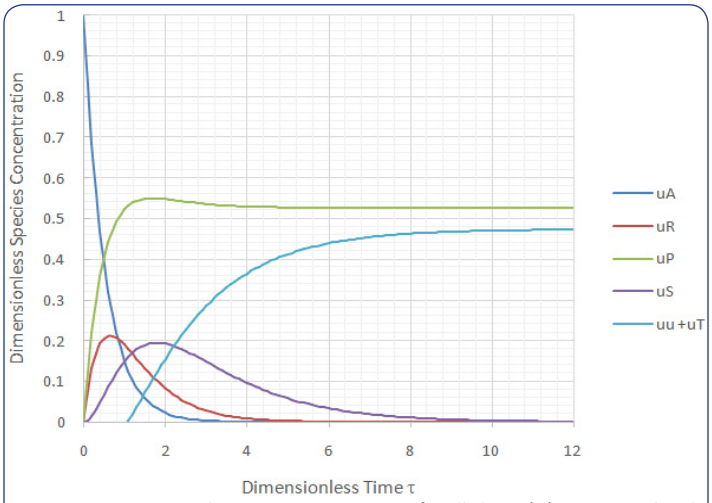

Figure 2: Dimensionless Concentrations of Cellulose (A), Activated Cellulose (R), Primary Tar (S), Primary Char (P) and Secondary Gas (T)+ Secondary Tar (U) as a Function of Dimensionless Time.

ω	0.8
β	2
κ	3
δ	1.33
ε	2.33
γ	1.33

Table 2

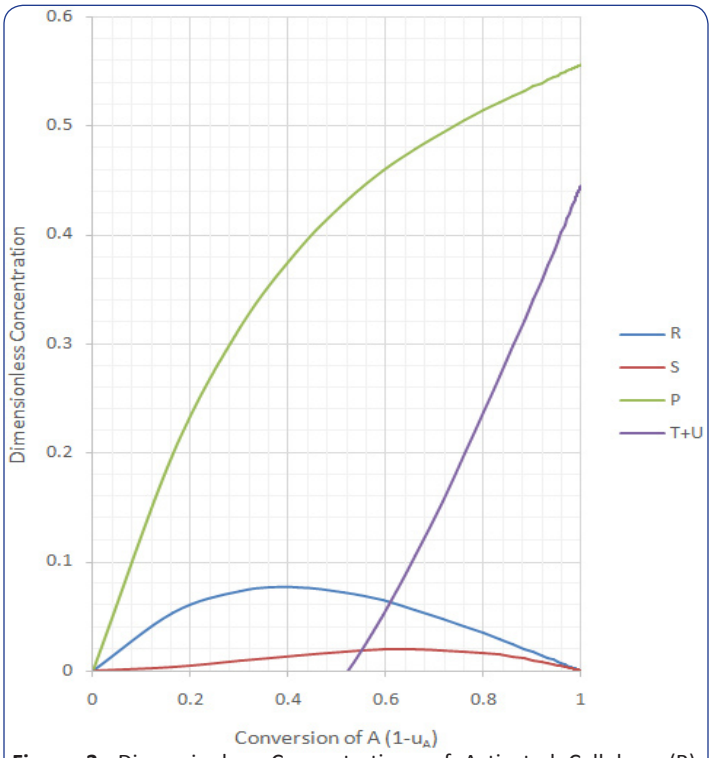

Figure 3: Dimensionless Concentrations of Activated Cellulose (R), Primary Tar (S), Primary Char (P) and Secondary Gas (T)+ Secondary Tar (U) as a Function of Conversion of Cellulose (A).

Conclusions

Biomass can be pyrolyzed into char, chemicals, bio-oil, and syn-gas.Computer simulations are used to study the kinetics of reactions that occur during pyrolysis of cellulose. The scheme of reactions that are believed to occur during pyrolysis of cellulose is given in Figure 1.0. The scheme of reactions shown in Figure 1.0 was modified from that proposed by Wooten et al. [4]. A is the cellulose, R is the activated cellulose, P is the product, S and U are the primary and secondary tar, and T is the secondary gas. The

secondary char from cellulose is formed from the polymerization of anhydrosugars, also called levoglucosan. Levoglucosan undergoes vapor phase polymerization. The kinetic rate expressions of the reactions shown in Figure 1.0 are given by Eqs. (1-6). The kinetic rate equations given by Eqs. [1-6] made dimensionless for the sixspecies and seven reaction rate constants. The state-space model for kinetic

Rate expressions are given by Eq. (14). The Eigen values are 0 thrice: $-(\varepsilon + \gamma)$, $-(\beta + \delta + \kappa)$, $-(1 + \omega)$. Negative signs for Eigen values indicate a stable system. Eqs. (8-13) can be solved for by the method of Laplace transforms. The model solutions are given by Eqs. (23-28).

The product distributions are shown in Figure 2.0 for a typical set of reaction rate constants. The intermediate product species, activated cellulose, R, and primary tar, S, can be seen to undergo a maximum concentration as a function of time. The concentration profile of species S is seen to be convexo-concave during the early times of formation. This has not been discussed before in the literature. The secondary tar and secondary gas begin to a lag time. The lag in species formation is a seminal finding. The concentration of product P is found to rise and found to reach an asymptotic plateau. The dimensionless concentration of species R, S, P, and T + U is plotted as a function of conversion of A in Figure 3.0.

References

1. MJ Antal, G Varhegyi (1995) Cellulose Pyrolysis Kinetics; The Current State of Knowledge. Ind. Eng. Chem. Res Vol 34(3): 708-717.
2. D Fengel (1969) The Ultrastructure of Cellulose from Wood. Wood Science and Technology 3(3): 203-271.
3. S Dimitru (2004) Polysaccharides: Structures Diversity and Functional Versatility (New York, NY: Marcell Dekker).
4. JB Wooten, JI Seeman, MR Hajaligol (2004) Observation and Characterization of Cellulose Pyrolysis Intermediates by 13C CPMAS NMR. A New Mechanistic Model. Energy and Fuels 18(1): 1–15.
5. X Bai, P Johnston, S Sadula, RC Brown (2013) Role of Levoglucosan Physiochemistry in Cellulose Pyrolysis. Journal of Analytical and Applied Pyrolysis 99: 58–65.
6. MJ Antal, Biomass Pyrolysis; A Review of the Literature Part 2 – Lignocellulose Pyrolysis in Advances in Solar Energy 175-255.
7. HS Mickley, TS Sherwood, CE Reed (1957) Applied Mathematical Methods in Chemical Engineering (New York, NY: McGraw Hill Professional).